ACS MATERIALS LETTERS

www.acsmaterialsletters.org

Letter

Catalyst-Free Dynamic Crosslinking of Polydicyclopentadiene via Thiol–Ene/Imine Chemistry

Published as part of ACS Materials Letters special issue "Sustainable Polymer Materials".

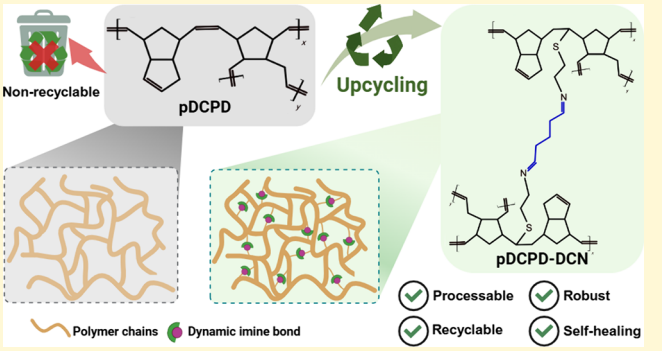
Leila Shahriari, Catherine Biju, Lillian N. Elam, Hayden E. Fowler, Yoongyeong Baek, Myungwoon Lee, Samuel C. Leguizamon, and Sungjin Kim*

Cite This: *ACS Materials Lett.* 2026, 8, 2807–2816

Read Online

ACCESS | Metrics & More | Article Recommendations | Supporting Information

ABSTRACT: The permanently crosslinked nature of thermosets fundamentally prevents recycling, creating persistent waste and environmental challenges. Among high-performance thermosets, polydicyclopentadiene (pDCPD) is widely used in transportation and infrastructure, yet most end-of-life material is landfilled or incinerated because its irreversibly crosslinked network resists conventional reprocessing. Here, pDCPD, a polynorbornene-based thermoset valued for its mechanical strength, chemical resistance, and compatibility with additive manufacturing, is upcycled into a dynamic covalent network (DCN) by introducing imine linkages. A two-step thiol–ene/imine sequence converts the permanent network into a (re)processable vitrimer-like material. Our dynamic pDCPD preserves high mechanical performance, exhibiting more than a 7-fold higher elastic modulus retention after recycling compared to its unmodified counterpart. Reversible imine chemistry also imparts intrinsic healing capability, reducing the incision width by ∼92% under simple, free-standing thermal treatment. This strategy establishes a practical route to convert pDCPD waste into DCNs, advancing sustainable thermoset design.



Global demand for polymer-based materials continues to rise, driven by their durability, lightweight design, energy-efficiency benefits, and ease of processing.[1,2] Thermosetting polymers account for approximately 65 million tons of annual production, representing nearly one-fifth of the total global polymer output by mass.[3] Thermoset polymers present significant challenges for recycling/upcycling compared with thermoplastics, arising from their permanently crosslinked covalent networks that necessitate harsh chemical or thermal conditions for depolymerization.[4−7] Consequently, most end-of-life thermoset polymers are still managed by incineration or landfilling, processes that heighten environmental concerns due to resource loss and potential pollutant generation.[8−10] Upcycling offers a valuable complementary strategy to address these limitations, involving the reprocessing of materials to impart enhanced properties, functionality, processability, or overall value, ideally within circularity.[11,12] Incorporating dynamic (reversible) covalent bonds into thermoset polymers yields dynamic covalent networks (DCNs) that enable efficient reprocessing, repair, and value-added upcycling, providing a promising route for end-of-life management while improving overall material sustainability.[13−25] Within these networks, the dynamic chemistries allow efficient bond exchanges under external stimuli (e.g., heat, pH, or light), or controlled bond cleavage enables the depolymerization of networks into valuable products that are amenable to closed-loop recycling and upcycling pathways.[4,15,26−33]

Polydicyclopentadiene (pDCPD) is a widely utilized thermoset polymer, recognized for its exceptional thermomechanical properties, impact resistance, and tunable material characteristics.[34−38] The unique combination of durability and low density makes pDCPD particularly attractive for transportation, construction, agriculture, energy, and defense sectors.[39−41] pDCPD is synthesized via ring-opening metathesis polymerization (ROMP) of dicyclopentadiene (DCPD), a process typically catalyzed by transition metal complexes such as molybdenum, tungsten, or ruthenium.[42−44] Recently, this chemistry has emerged as a versatile strategy in the additive manufacturing (AM) of robust, intricate, high-resolution structures that are unattainable through conventional processing

Received: July 29, 2026
Revised: August 12, 2026
Accepted: August 13, 2026
Published: August 25, 2026



ACS Publications

© 2026 The Authors. Published by American Chemical Society

Downloaded from pubs.acs.org/amlcef/article-pdf/8/9/2807/6740807/tz-2026-00833d.pdf by FLORIDA STATE UNIV user on 02 November 2026

techniques.[45,46] Despite the impressive mechanical, thermal, and chemical stability that makes pDCPD so valuable, these same attributes hinder its recyclability, leading to the buildup of persistent, non-degradable waste.[8,39,47] To address this challenge, several dynamic bonding motifs have been recently incorporated into pDCPD networks, including Diels–Alder,[48] silyl ether,[41,49,50] and boronic ester linkages,[37] to impart reprocessability via dissociative or associative pathways. In dissociative systems such as Diels–Alder adducts, bonds must first cleave before reassociating, whereas associative silyl ether and boronic ester vitrimers rely on bond-exchange reactions that typically require added catalysts or tailored comonomers for efficient stress relaxation. Compared to pDCPD vitrimers that require such comonomer reformulation and catalysts, our postsynthetic approach achieves comparable reprocessability with a simpler, catalyst-/additive-free workflow, in which imine bonds, particularly those that undergo transimination, provide catalyst-free, associative bond exchange and robust environmental tolerance.[51,52] Dynamic imine chemistry stands out as one of the most well-studied approaches, offering an adaptable and efficient method for polymer functionalization, while enabling reprocessability, malleability, and self-healability without dissociating bonds that compromise network stability.[53−59]

Here, we present a chemical strategy for upcycling additively manufactured pDCPD by introducing dynamic imine linkages to construct DCNs capable of associative transimination (Figure 1). This design addresses the persistent challenge of pDCPD waste recycling/upcycling by enabling associative network rearrangement, effectively converting a permanently crosslinked thermoset into a reprocessable vitrimer-like material. Unlike prior approaches that require substantial reformulation, this design activates reversible network rearrangement with minimal modification to the parent thermoset, without using

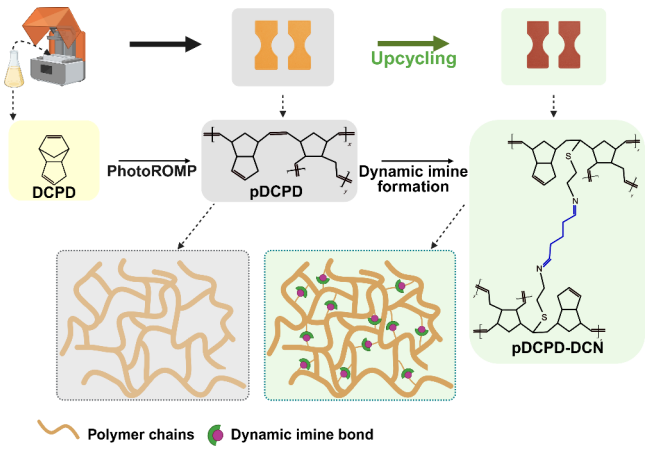


Figure 1. Schematic illustration of the chemical upcycling design that transforms a 3D-printed polydicyclopentadiene (pDCPD) thermoset into a dynamic covalent network (pDCPD-DCN) through the incorporation of dynamic imine linkages. The pDCPD network is first generated by stereolithography (SLA) of a dicyclopentadiene (DCPD) resin via photoinduced ring-opening metathesis polymerization (PhotoROMP), followed by dynamic imine formation to convert the irreversible thermoset into a reprocessable DCN. The structure shown for pDCPD-DCN depicts modification along the main chain for simply representing the reaction chemistry; we note that the thiol–ene and imine-forming reactions can occur at multiple unsaturated C=C sites at different locations, including the main backbone, pendant chains, and cycloalkenes, to yield a dynamic network.

catalysts or additives to dissociate the existing network structure of pDCPD. The resulting networks exhibit efficient recyclability and reprocessability over multiple cycles while preserving excellent structural integrity. Beyond imparting malleability and healing, integrating imine linkages into the pDCPD polymer backbone also improves its mechanical strength, demonstrating that dynamic covalent chemistry can deliver both robustness and circularity simultaneously. These results highlight a generalizable route for upcycling pDCPD and underscore the potential of imine-based DCNs to advance sustainable thermoset technologies that support circular material lifecycles.

Stereolithography (SLA)-printed pDCPD (pDCPD-pristine) was chemically upcycled via a sequential dynamic covalent modification process, analogous to approaches reported for ABS-vitrimers by Kim et al.[59] We leveraged the unsaturated double bonds inherently within pDCPD networks for thiol–ene, "click" chemistry,[60−62] enabling attachment of cysteamine and thereby introducing primary amine functionalities. The amine-functionalized polymer (pDCPD-amine) was subsequently reacted with glutaraldehyde crosslinker, a short-chain dialdehyde, to induce dynamic imine bond formation, yielding the targeted pDCPD-DCNs (pDCPD-imine) (see Supporting Information, Experimental Section 1.4 for more details), as illustrated in Figure 2a,b. The incorporation of the thiol–ene step and subsequent imine formation within the 3D-printed samples was supported by solid-state NMR (ssNMR) spectroscopy (Figure 2c). The ssNMR spectra showed a pronounced decrease in olefinic carbon signals (~120 ppm),[63] suggesting consumption of unsaturated double bonds in pendant chains during the thiol–ene reaction. The three spectra showed a resonance at ~131.6 ppm, which is assigned to overlapping unsaturated C=C sites in the main backbone and cyclopentene rings.[64−66] Because this resonance is the most prominent shared peak across all three samples, we used it as a common reference for spectral comparison. Concurrently, an increased intensity in the aliphatic carbon region (30–60 ppm)[64−66] was observed for pDCPD-amine, consistent with the incorporation of the cysteamine linker. Following imine formation, pDCPD-imine exhibited a further increase in aliphatic signal intensity compared to pDCPD-amine, reflecting additional aliphatic carbon contributions from the aldehyde-derived crosslinker functionalities. Notably, the feature at ~39.5 ppm, assigned to the cysteamine-derived C–N linkage,[67] increased from pDCPD-pristine to pDCPD-amine and remained largely unchanged upon conversion to pDCPD-imine, supporting retention of the cysteamine-derived C–N linkage during subsequent imine formation. Complementary Fourier-transform infrared (FTIR) analysis further supports functionalization at multiple unsaturated sites within the pDCPD network (Figure S1). The FTIR band at ~972 cm^{-1} is assigned to bending vibrations of trans C=CH units in acyclic diene segments (main backbone and pendant chains), whereas the band near 754 cm^{-1} corresponds to C=CH vibrations of cyclopentene rings.[64,66,68,69] After thiol–ene functionalization and imine formation, the intensities of both bands decreased, consistent with consumption of unsaturated sites in the backbone, pendant chains, and cyclopentene rings. Collectively, these spectroscopic observations support successful thiol–ene modification and subsequent imination, consistent with the desired dynamic network formation.

Network changes induced by the introduction of a low concentration of dynamic imine bonds were quantified by swelling

Downloaded from pubs.acs.org/amlcef/article-pdf/8/9/2807/6740807/tz-2026-00833d.pdf by FLORIDA STATE UNIV user on 02 November 2026

https://doi.org/10.1021/acsmaterialslett.6c00833
ACS Materials Lett. 2026, 8, 2807−2816

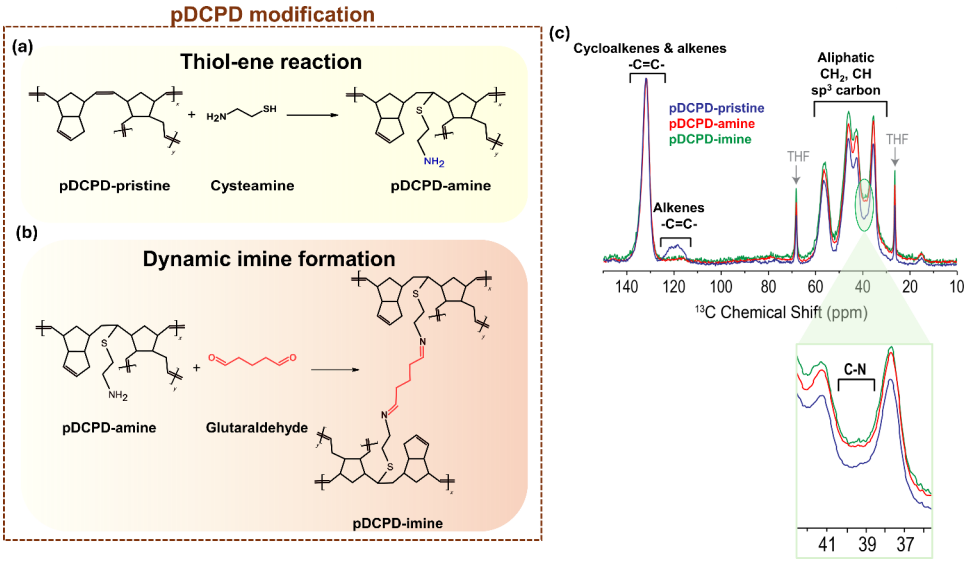


Figure 2. Schematic illustration of the sequential thiol–ene/imine functionalization from SLA-printed pDCPD-pristine to dynamic covalent pDCPD-imine networks. (a) Thiol–ene functionalization of pDCPD-pristine to introduce amine functionality using cysteamine to produce pDCPD-amine, followed by (b) imine formation with glutaraldehyde to yield pDCPD-imine. The structures are shown as a representative example of network modification for simplicity. We note that the thiol–ene reactions can take place at multiple alkene (C=C) sites within the network, including the main backbone, pendant chains, and cycloalkenes (Figure S1). (c) One-dimensional solid-state ^{13}C cross-polarization (1D ss ^{13}C CP NMR) spectra are shown for pDCPD-pristine (blue), pDCPD-amine (red), and pDCPD-imine (green). All spectra were normalized to the C=C resonance at 131.6 ppm, which is assigned to unsaturated carbon sites in the main backbone and cyclopentene rings, to facilitate comparison of the aliphatic region (30–60 ppm).[64–66] A resonance in the olefinic region at ∼120 ppm is assigned to alkenes in the pendant chains.[63] Residual solvent peaks (THF used in the synthesis) are marked by gray arrows. An expanded view (highlighted in green) of the aliphatic region centered at ∼39.5 ppm shows increased signal intensity in pDCPD-amine and pDCPD-imine relative to pDCPD-pristine. This resonance is consistent with the C–N environment introduced during the thiol–ene step and retained upon imine formation.[67]

measurements and the Flory–Rehner analysis to determine the crosslink density (x) of the networks (see Supporting Information, eqs 1–5).[70–72] As shown in Figure 3a and Table S1, conversion of pDCPD-pristine to pDCPD-amine increased the crosslink density from 1.55 ± 0.03 to 1.71 ± 0.05 mmol cm^{-3}. This enhancement could be attributed to the generation of primary amine groups following consumption of C=C bonds via thiol–ene addition, promoting additional branching and entanglement-like topological constraints, thereby yielding a more compact network.[73] This densification is also likely promoted by the presence of secondary interactions, particularly hydrogen bonding between amine groups and the pDCPD backbone, which tighten the swollen network.[74,75] Introduction of dynamic imine crosslinks via reaction of pDCPD-amine with dialdehyde led to the highest crosslink density (1.85 ± 0.04 mmol cm^{-3}), confirming the formation of effective covalent imine linkages that enable reversible network rearrangement.[52] The mechanical integrity of the swollen networks was further evaluated by gravity-induced deformation after 24 h of immersion in tetrahydrofuran (THF). The pDCPD-pristine exhibited pronounced bending (Figure 3b), consistent with its relatively low crosslink density and limited resistance to swelling. By comparison, pDCPD-amine showed diminished bending, reflecting a tighter network with enhanced interchain interactions, such as hydrogen bonding and other physical associations. Remarkably, the pDCPD-imine sample demonstrated minimal deflection under gravitational load, highlighting the reinforced stiffening effect achieved by the addition of dynamic imine crosslinks. These reversible, yet mechanically robust, covalent crosslinks significantly enhance matrix stiffness and uphold structural integrity even in solvent-swollen conditions.[76,77] Mechanical properties of the networks were evaluated by tensile testing (Figure S2 and Table S2). The pDCPD-imine network displayed a higher ultimate tensile strength (UTS ∼ 21.23 ± 3.10 MPa) than pDCPD-pristine (19.91 ± 1.63 MPa). Notably, the Young's moduli (E) of all networks remained comparably similar (E(pDCPD-pristine) = 1.02 GPa and E(pDCPD-imine) = 1.18 GPa), as shown in Figure S2. This similarity arises because the elastic modulus reflects the intrinsic stiffness of the polymer network in the initial, small-strain region, determined by factors such as backbone rigidity and local segmental flexibility.[78,79] The low fraction of dynamic imine incorporation chiefly reinforces large-scale network cohesion and ultimate strength, rather than altering the local stiffness of chain segments, so the modulus is relatively unaffected unless extensive modification occurs at the segmental level.[80]

The viscoelastic behavior of the networks was examined at 140 °C above the glass transition temperatures (T_g) of the pDCPD (Figure S3), revealing distinct differences between pDCPD-pristine and its imine-functionalized analog, pDCPD-imine (Figure 4a,b). While both materials demonstrated an increase in storage modulus (E') across the measured frequency range (0.1–100 Hz), indicative of highly crosslinked glassy thermosets,[27,81] the pDCPD-imine exhibited a slightly lower E' than the unmodified pDCPD (Figure 4a). At high frequencies, the oscillation period is much shorter than the intrinsic timescale of imine bond exchange at the measurement temperature, so these dynamic bonds are effectively frozen during the oscillatory deformation, and the viscoelastic response is governed primarily

https://doi.org/10.1021/acsmaterialslett.6c00833
ACS Materials Lett. 2026, 8, 2807−2816

Downloaded from pubs.acs.org/amlcef/article-pdf/8/9/2807/6740807/tz-2026-00833d.pdf by FLORIDA STATE UNIV user on 02 November 2026

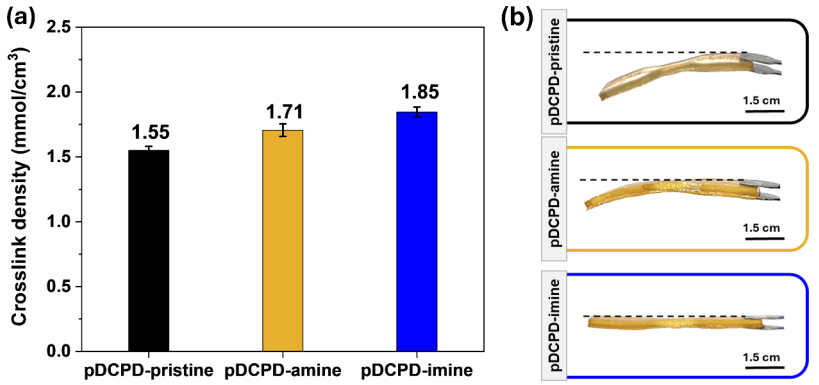


Figure 3. (a) Crosslink density of pDCPD-pristine, pDCPD-amine, and pDCPD-imine networks. (b) Photographs of the gravity-induced deformation of dog-bone specimens after 24 h of swelling in THF.

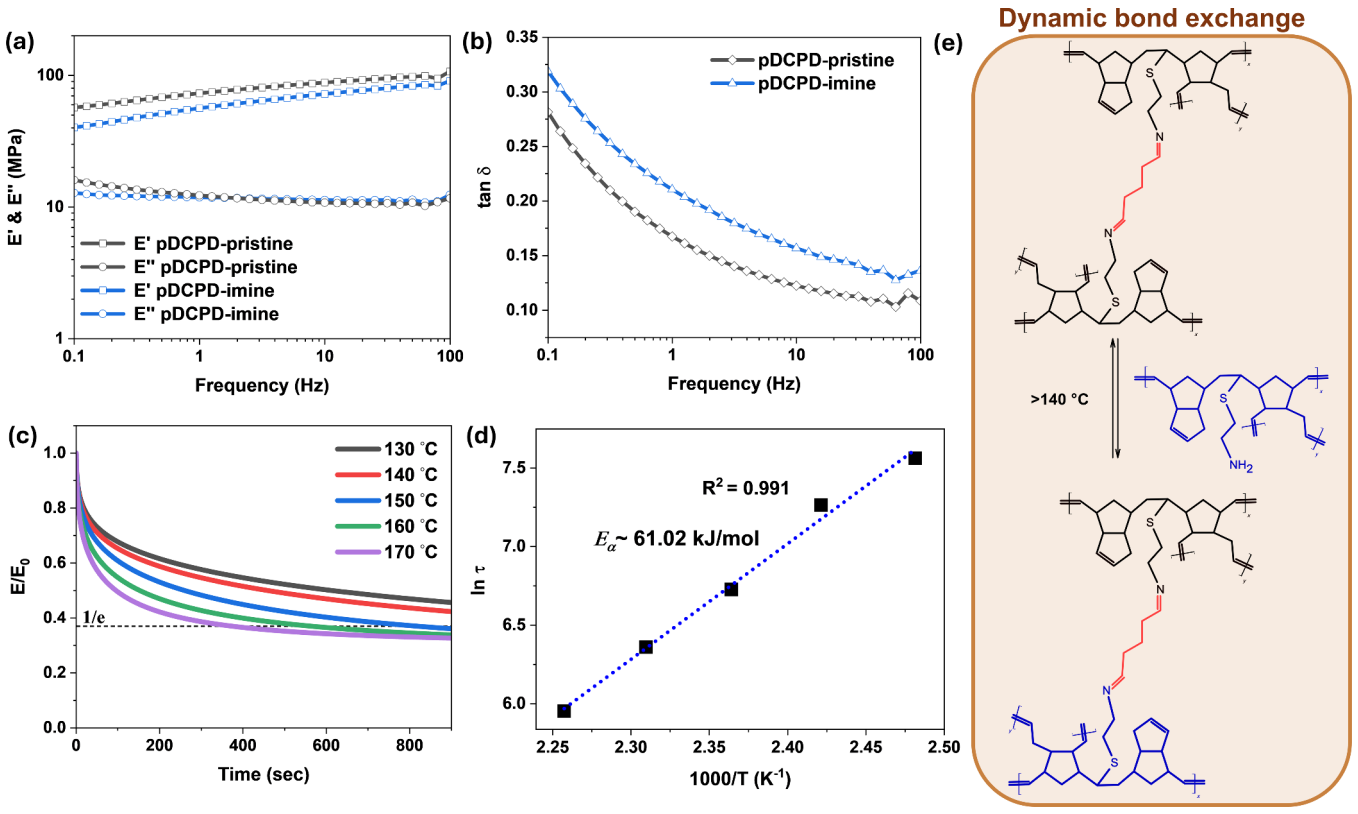


Figure 4. Rheological characterization of the pDCPD-networks. (a) Frequency-dependent storage (E') and loss moduli (E'') of pDCPD-pristine and pDCPD-imine at 140 °C measured by tensile DMA (1% strain, 0.1–100 Hz). (b) Corresponding loss factor ($\tan\delta = E''/E'$) calculated from the data in (a). (c) Stress-relaxation behavior of pDCPD-imine (1% strain) recorded for 900 s between 130 and 170 °C in 10 °C increments with DMA. (d) Relaxation times (τ) were determined at the point where the normalized relaxation modulus (E/E_0) decayed to ($1/e$) ~37% of its initial value, consistent with a Maxwell-type viscoelastic response (see Supporting Information, Experimental Section 2.5). (d) Arrhenius analysis of τ obtained from the stress-relaxation profiles in (c), yielding an E_a of ~61 kJ/mol (see Supporting Information, Experimental Section 2.5 and Table S3 for details). (e) Schematic representation of dynamic imine exchange (transimination) within the pDCPD-imine network. The structure shown for dynamic bond exchange illustrates modification along the main chain only as a simplified representation of the reaction chemistry as we stated in Figure 2 reaction schemes.

by the underlying network architecture and effective crosslink density, rather than by bond exchange events.[82] Under these conditions, the E' of pDCPD-imine remains slightly lower than that of pDCPD-pristine, even though equilibrium swelling measurements indicate a higher overall crosslink density for pDCPD-imine (Figure 3a). We attribute this behavior to increased local segmental mobility introduced by the thiol–ene and imine-containing linkers that create more flexible

https://doi.org/10.1021/acsmaterialslett.6c00833
ACS Materials Lett. 2026, 8, 2807−2816

Downloaded from pubs.acs.org/amlcef/article-pdf/8/9/2807/6740807/1tz-2026-00833d.pdf by FLORIDA STATE UNIV user on 02 November 2026

segments within the otherwise rigid pDCPD network and reduce the stiffness of the network strands.[83] The higher loss tangent (tan δ) for the pDCPD-imine network signifies greater viscous damping and enhanced energy dissipation, consistent with active bond exchange that couples robust elasticity with efficient stress relaxation (Figure 4b).[84,85] Such characteristics exemplify the advantages of dynamic covalent networks, where bond rearrangement continuously allows efficient stress relaxation even in systems with substantial crosslink densities, provided the exchangeable bonds remain labile at the applied temperature.[86,87]

Stress-relaxation experiments further support vitrimer-like behavior, with relaxation times (τ) obtained at different temperatures following an Arrhenius dependence (Figure 4c, see Supporting Information eqs 6 and 7), defining a characteristic of vitrimer networks.[6,59,88–93] The temperature dependence of τ yields an apparent activation energy (E_a) of approximately 61 kJ/mol (Figure 4d and Table S3), in line with previously reported polyimine-based vitrimers.[51,76,80,94–96] From this analysis, the topology-freezing transition temperature (T_v) is estimated to be around ∼98 °C (see Supporting Information, eq 8 and Table S4), defining the threshold above which dynamic bond exchange becomes operational, and bond exchange proceeds efficiently.[97–99] Accordingly, dynamic transimination is expected to proceed efficiently over the experimental temperature range of 130–170 °C, as illustrated in Figure 4e, enabling reprocessing and healing while preserving mechanical strength at service conditions below this temperature.

Permanently crosslinked polymers are inherently resistant to reshaping or recycling because their network topology is fixed.[15,20,28,100] In contrast, the pDCPD-imine network reported here incorporates dynamic imine linkages that undergo associative bond exchange, enabling topological rearrangement without bulk depolymerization.[51,58,59] To demonstrate its reprocessability/recyclability, strip-shaped specimens were subjected to a thermal compression process, followed by dynamic mechanical analysis (DMA). Whereas pDCPD-pristine (R-I) showed minimal fusion and retained distinct interfaces between compressed fragments, the pDCPD-imine (R-I) exhibited substantially improved interfacial cohesion, evidencing efficient network reconstruction across fragment boundaries (Figure 5a). As shown in Figure 5b,c, the reprocessed pDCPD-imine (R-I) specimen retains approximately 87% of its initial storage modulus, decreasing modestly from ∼1120 MPa (pDCPD-imine (R-0)) to ∼975 MPa. This high modulus retention highlights the efficiency of the dynamic imine exchange in reconstructing network connectivity across fractured interfaces, thereby preserving mechanical robustness upon recycling.[59,76,101] By contrast, pDCPD-pristine experiences a drastic decline in stiffness, with its storage modulus falling from ∼1360 MPa (pDCPD-pristine (R-0)) to ∼163 MPa (≈12% retention), reflecting the inherent inability of its static

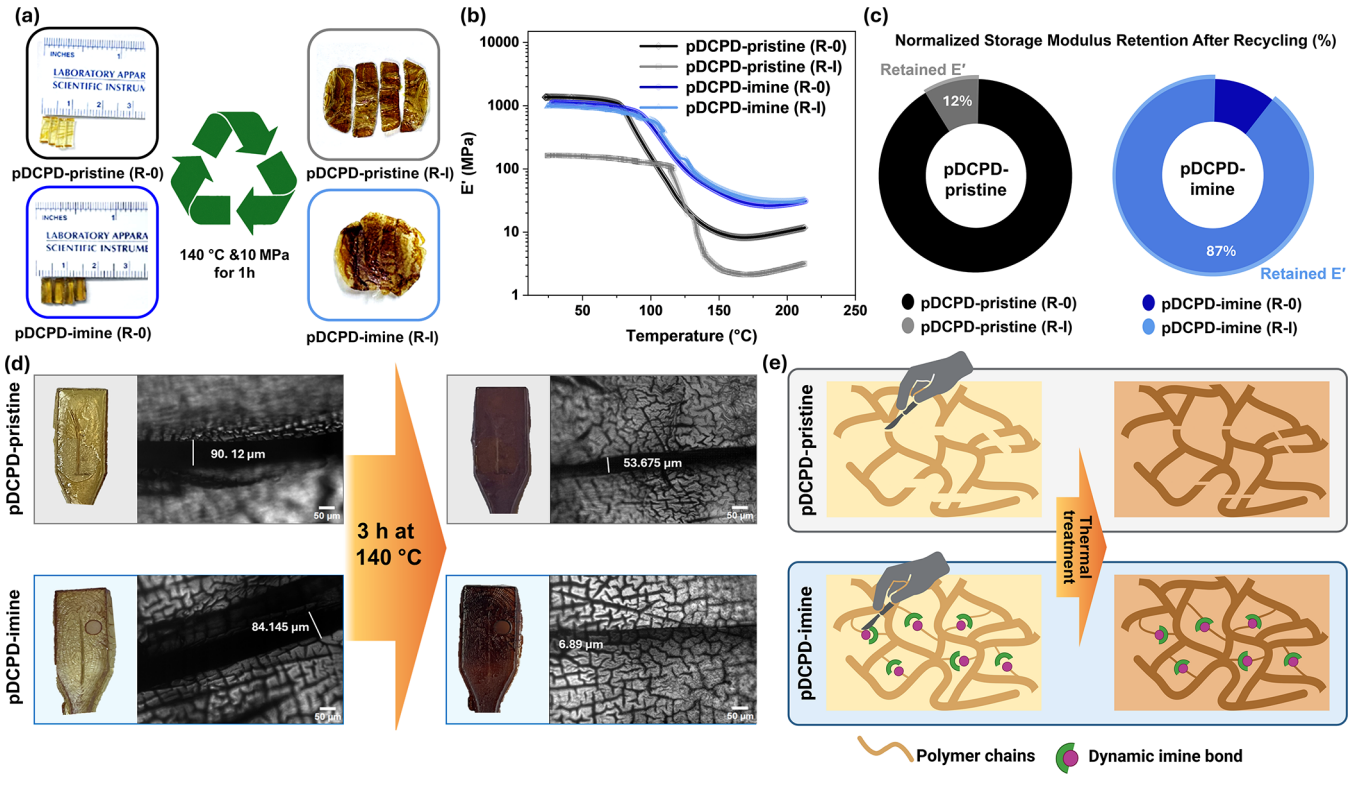


Figure 5. (a) Photos of strip-shaped pDCPD-pristine and pDCPD-imine specimens before recycling (R-0) and after thermal compression at 140 °C under 10 MPa for 1 h (R-I). (b) DMA curves of the same specimens corresponding to the processing conditions described in (a). (c) Donut plots showing normalized storage modulus retention (E'/E'(R-0)) of pristine and imine-modified pDCPD networks after recycling (R-I). The pristine network retains 12% of its original storage modulus, whereas the imine-modified network retains 87% after recycling. Retention values are calculated based on the normalized storage modulus data shown in (b). (d) Photos and optical microscopic images of pDCPD-pristine and pDCPD-imine samples subjected to an incision before and after thermal healing at 140 °C for 3 h under vacuum. (e) Schematic representation of self-healing in the pDCPD-imine network, where reversible dynamic imine exchange enables network rearrangement and crack closure with thermal treatment compared to the pDCPD-pristine with permeant network.

Downloaded from pubs.acs.org/amlcef/article-pdf/8/9/2807/6740807/tz-2026-00833d.pdf by FLORIDA STATE UNIV user on 02 November 2026

https://doi.org/10.1021/acsmaterialslett.6c00833
ACS Materials Lett. 2026, 8, 2807−2816

covalent network to recover mechanical integrity after these treatments.[28,100,102]

The recyclability of the DCNs was further evaluated over three consecutive thermal reprocessing compression cycles (R-I to R-III) at 140 °C and 10 MPa (Figure S4a). Across these cycles, the storage modulus exhibited variations within the same order of magnitude, demonstrating that pDCPD–imine retains its elastic properties under repeated reprocessing with insignificant mechanical degradation, consistent with reported behavior for imine-based vitrimers (Figure S4b,c).[51,59,76,103−105] However, the slight reduction aligns with the expected behavior of dynamic covalent systems exposed to multiple processing cycles, in which network fatigue and side reactions can cumulatively produce modest reductions in stiffness.[106,107] A slight increase in storage modulus was observed after the second reprocessing (R-II), suggesting that additional thermal treatment can promote further dynamic bond exchange and network reorganization, potentially leading to more effective crosslink rearrangement or incremental densification.[108]

Thermal healing experiments further highlight the distinct responses of pristine and dynamic networks. Figure 5d and Table S5 compare incision closure in pDCPD-pristine and pDCPD-imine before and after contact-free heat treatment at 140 °C in a vacuum oven. In pDCPD-pristine, the incision width decreased only from 90.12 ± 1.03 to 53.68 ± 1.05 μm (corresponding to ∼40% healing), reflecting partial narrowing driven by rubbery-state viscous flow and limited polymer-chain interpenetration above T_g, but not true network reconstruction.[82,109,110] In contrast, the pDCPD-imine material displayed nearly complete closure of the incision, with the width shrinking from 84.15 ± 1.48 to 6.89 ± 0.91 μm, corresponding to ∼92% healing. This pronounced recovery is attributed to dynamic imine linkages that undergo transimination, enabling reversible bond exchange and local network reconnection across the cut (Figure 5e).[111−114] The resulting restoration of structural continuity exemplifies vitrimer-like thermal healing, in which associative bond exchange allows simultaneous maintenance of crosslink density and efficient repair of macroscopic damage without the need for additives or solvents.[23,27,28,82,99]

This work establishes a simple yet practical strategy for upcycling additively manufactured thermoset pDCPD into robust and reprocessable materials through the incorporation of dynamic imine crosslinks without using catalysts or dissociating the network. Our thiol–ene click reaction followed by imine formation/transimination approach activates associative network rearrangement. This enables efficient recycling and reshaping while preserving the excellent mechanical performance characteristic of the parent thermoset, as evidenced by ∼87% retention of the elastic modulus after reprocessing (>7× the ∼12% retention for pDCPD-pristine) and 92% healing of an imposed incision. The ability to impart vitrimer-like behavior to pDCPD highlights a broadly applicable design principle for advancing circularity in other high-performance thermosets via simple modification of chemical formulation or post-printing treatments. Importantly, this platform offers opportunities for further property tuning by increasing the fraction of dynamic bonds or by integrating imine chemistry with other compatible vitrimer systems. Our findings demonstrate that dynamic covalent chemistry can be seamlessly incorporated to upcycle high-performance engineering thermosets into healable, recyclable networks while preserving mechanical integrity, offering a pathway toward sustainable polymer manufacturing.

■ ASSOCIATED CONTENT

Supporting Information

The Supporting Information is available free of charge at https://pubs.acs.org/doi/10.1021/acsmaterialslett.6c00833.

Experimental section: materials, methods, and characterizations, including Figures S1–S4 and Tables S1–S5 (PDF)

■ AUTHOR INFORMATION

Corresponding Author

Sungjin Kim – *Department of Chemical and Biological Engineering, University of New Mexico, Albuquerque, New Mexico 87131, United States;* orcid.org/0000-0002-2068-9189; Email: sungjinkim@unm.edu

Authors

Leila Shahriari – *Department of Chemical and Biological Engineering, University of New Mexico, Albuquerque, New Mexico 87131, United States;* orcid.org/0009-0002-7442-0270

Catherine Biju – *Department of Chemical and Biological Engineering, University of New Mexico, Albuquerque, New Mexico 87131, United States*

Lillian N. Elam – *Department of Chemical and Biological Engineering, University of New Mexico, Albuquerque, New Mexico 87131, United States; Sandia National Laboratories, Albuquerque, New Mexico 87185, United States*

Hayden E. Fowler – *Sandia National Laboratories, Albuquerque, New Mexico 87185, United States*

Yoongyeong Baek – *Department of Chemistry, Drexel University, Philadelphia, Pennsylvania 19104, United States*

Myungwoon Lee – *Department of Chemistry, Drexel University, Philadelphia, Pennsylvania 19104, United States;* orcid.org/0000-0001-9230-0446

Samuel C. Leguizamon – *Sandia National Laboratories, Albuquerque, New Mexico 87185, United States; Savannah River National Laboratory, Aiken, South Carolina 29808, United States;* orcid.org/0000-0003-3395-6562

Complete contact information is available at: https://pubs.acs.org/doi/10.1021/acsmaterialslett.6c00833

Author Contributions

L.S. performed the DMA properties after each reprocessing cycle, the quantitative analysis of the rheological data, and wrote the main manuscript. C.B. performed synthetic upcycling, FTIR, swelling measurement, recycling, and self-healing assessments. L.N.E. and S.C.L. synthesized the pDCPD and 3D-printed specimens using SLA and performed tensile and DMA measurements. H.E.F. performed the rheological and mechanical characterization. Y.B. and M.L. performed the ssNMR characterization. S.K. and S.C.L. conceived the idea and acquired funding. L.S. and S.K. wrote the manuscript with contributions from all authors. All authors have reviewed and approved the final version of the manuscript.

Notes

The authors declare that the following patents related to this work have been filed: U.S. Patent Application. No. 63/846,607.

Downloaded from pubs.acs.org/amlcef/article-pdf/8/9/2807/6740807/tz-2026-00833d.pdf by FLORIDA STATE UNIV user on 02 November 2026

https://doi.org/10.1021/acsmaterialslett.6c00833
ACS Materials Lett. 2026, 8, 2807−2816

■ ACKNOWLEDGMENTS

This research was supported by the Sandia Laboratory Directed Research & Development (LDRD) - Award ID 2581603 (Sponsor 100001011 - National Technology & Engineering Solutions of Sandia LLC) and startup funding from the Department of Chemical and Biological Engineering at the University of New Mexico. This work was in part produced by the Battelle Savannah River Alliance, LLC under contract number 89303321CEM000080 with the U.S. Department of Energy (SCL). Publisher acknowledges the U.S. Government license to provide public access under the DOE Public Access Plan (http://energy.gov/downloads/doe-public-access-plan). This work was supported by the Laboratory Directed Research and Development (LDRD) program within the Savannah River National Laboratory (SRNL). The authors acknowledge the use of facilities at the Advanced Materials Laboratory (UNM/SNL). The authors thank Dr. Nick J Carroll and Dr. Gabriel P. López for optical microscopy. We thank Drs. Ivan Hung and Zhehong Gan at the National High Magnetic Field Laboratory for their assistance with ssNMR experiments. The National High Magnetic Field Laboratory is supported by the National Science Foundation through NSF/DMR-2128556 and the State of Florida. ssNMR characterization was supported by the NIH grant NS139178 to M.L. The authors acknowledge training from Danielle J. Chun in pDCPD purification; Ashley Garcia and Carina Anastasio in optical microscopy; and Geoffrey Courtin in laboratory safety. The authors used Perplexity AI to improve the manuscript's readability and language, then thoroughly reviewed and edited the content and take full responsibility for the published article. Figures 1, 5e, and the TOC were created in https://BioRender.com.

■ REFERENCES

(1) Phiri, R.; Mavinkere Rangappa, S.; Siengchin, S.; Oladijo, O. P.; Ozbakkaloglu, T. Advances in Lightweight Composite Structures and Manufacturing Technologies: A Comprehensive Review. *Heliyon* **2024**, *10*, e39661.

(2) Houssini, K.; Li, J.; Tan, Q. Complexities of the Global Plastics Supply Chain Revealed in a Trade-Linked Material Flow Analysis. *Commun. Earth Environ.* **2025**, *6*, 257.

(3) Geyer, R.; Jambeck, J. R.; Law, K. L. Production, Use, and Fate of All Plastics Ever Made. *Sci. Adv.* **2017**, *3*, e1700782.

(4) Fortman, D. J.; Brutman, J. P.; De Hoe, G. X.; Snyder, R. L.; Dichtel, W. R.; Hillmyer, M. A. Approaches to Sustainable and Continually Recyclable Cross-Linked Polymers. *ACS Sustain. Chem. Eng.* **2018**, *6*, 11145–11159.

(5) Singh, N.; Walker, T. R. Plastic Recycling: A Panacea or Environmental Pollution Problem. *Npj Mater. Sustain.* **2024**, *2*, 17.

(6) Lessard, J. J.; Stewart, K. A.; Sumerlin, B. S. Controlling Dynamics of Associative Networks through Primary Chain Length. *Macromolecules* **2022**, *55*, 10052–10061.

(7) Stewart, K. A.; Le, T. H.; Wei, N. B.; Cantor, A. J.; Rynk, J. F.; Sumerlin, B. S. Biobased Polystyrene Vitrimers for Thermoset Circularity. *ACS Appl. Polym. Mater.* **2024**, *6*, 13034–13041.

(8) Post, W.; Susa, A.; Blaauw, R.; Molenveld, K.; Knoop, R. J. I. A Review on the Potential and Limitations of Recyclable Thermosets for Structural Applications. *Polym. Rev.* **2020**, *60*, 359–388.

(9) Schneiderman, D. K.; Hillmyer, M. A. 50th Anniversary Perspective: There Is a Great Future in Sustainable Polymers. *Macromolecules* **2017**, *50*, 3733–3749.

(10) Long, T. E. Toward Recyclable Thermosets. *Science* **2014**, *344*, 706–707.

(11) Jehanno, C.; Alty, J. W.; Roosen, M.; Meester, S., De; Dove, A. P.; Chen, E. Y.-X.; Leibfarth, F. A.; Sardon, H. Critical Advances and Future Opportunities in Upcycling Commodity Polymers. *Nature* **2022**, *603*, 803–814.

(12) Goring, P. D.; Priestley, R. D. Polymer Recycling and Upcycling: Recent Developments toward a Circular Economy. *JACS Au* **2023**, *3*, 2609–2611.

(13) Wojtecki, R. J.; Meador, M. A.; Rowan, S. J. Using the Dynamic Bond to Access Macroscopically Responsive Structurally Dynamic Polymers. *Nat. Mater.* **2011**, *10*, 14–27.

(14) Deng, Y.; Zhang, Q.; Feringa, B. L.; Tian, H.; Qu, D.-H. Toughening a Self-Healable Supramolecular Polymer by Ionic Cluster-Enhanced Iron-Carboxylate Complexes. *Angew. Chem., Int. Ed.* **2020**, *59*, 5278–5283.

(15) Samanta, S.; Kim, S.; Saito, T.; Sokolov, A. P. Polymers with Dynamic Bonds: Adaptive Functional Materials for a Sustainable Future. *J. Phys. Chem. B* **2021**, *125*, 9389–9401.

(16) Capelot, M.; Montarnal, D.; Tournilhac, F.; Leibler, L. Metal-Catalyzed Transesterification for Healing and Assembling of Thermosets. *J. Am. Chem. Soc.* **2012**, *134*, 7664–7667.

(17) Chen, C.-W.; Mao, H.-I.; Lee, H.-K.; Chou, J.-Y.; Rwei, S.-P. Upcycling Recycled Epoxy-Based Vitrimer for Enhancing Toughness of Poly(Ethylene Terephthalate). *J. Polym. Environ.* **2024**, *32*, 621–631.

(18) Kong, L.; Wu, R.; Zhang, J.; Huang, S.; Xie, Z.; Wu, J. High Performance, Self-Adhesive and Recyclable Dynamic Crosslinked Waste Rubber Particle Blends toward Upcycling of Waste Rubber. *Green Chem.* **2024**, *26*, 1523–1532.

(19) Morado, E. G.; Paterson, M. L.; Ivanoff, D. G.; Wang, H.-C.; Johnson, A.; Daniels, D.; Rizvi, A.; Sottos, N. R.; Zimmerman, S. C. End-of-Life Upcycling of Polyurethanes Using a Room Temperature, Mechanism-Based Degradation. *Nat. Chem.* **2023**, *15*, 569–577.

(20) Yue, L.; Bonab, V. S.; Yuan, D.; Patel, A.; Karimkhani, V.; Manas-Zloczower, I. Vitrimerization: A Novel Concept to Reprocess and Recycle Thermoset Waste via Dynamic Chemistry. *Glob. Chall.* **2019**, *3*, 1800076.

(21) Yan, P.; Zhao, W.; Fu, X.; Liu, Z.; Kong, W.; Zhou, C.; Lei, J. Multifunctional Polyurethane-Vitrimers Completely Based on Transcarbamoylation of Carbamates: Thermally-Induced Dual-Shape Memory Effect and Self-Welding. *RSC Adv.* **2017**, *7*, 26858–26866.

(22) Fortman, D. J.; Sheppard, D. T.; Dichtel, W. R. Reprocessing Cross-Linked Polyurethanes by Catalyzing Carbamate Exchange. *Macromolecules* **2019**, *52*, 6330–6335.

(23) He, Y.; Ma, M.; Li, L.; Li, Z.; Zhao, S.; Zhao, X.; Advincula, R.; Tian, M.; Gao, S.; Yang, H.; Cao, P.-F. Hybrid Dynamic Covalent Network as a Protective Layer and Solid-State Electrolyte for Stable Lithium-Metal Batteries. *ACS Appl. Mater. Interfaces* **2023**, *15*, 23765–23776.

(24) Lu, Y.-X.; Guan, Z. Olefin Metathesis for Effective Polymer Healing via Dynamic Exchange of Strong Carbon–Carbon Double Bonds. *J. Am. Chem. Soc.* **2012**, *134*, 14226–14231.

(25) Ma, Y.; Stellacci, F. Structure–Property Relationships of Elastomeric Vinylogous Urethane Thermosets and Their Application as Closed-Loop Recyclable Strain Sensors. *Macromolecules* **2025**, *58*, 1923–1934.

(26) Zou, W.; Dong, J.; Luo, Y.; Zhao, Q.; Xie, T. Dynamic Covalent Polymer Networks: From Old Chemistry to Modern Day Innovations. *Adv. Mater.* **2017**, *29*, 1606100.

(27) Kloxin, C. J.; Bowman, C. N. Covalent Adaptable Networks: Smart, Reconfigurable and Responsive Network Systems. *Chem. Soc. Rev.* **2013**, *42*, 7161–7173.

(28) Shahriari, L.; Kim, S. Toward Circular Polymer Materials and Manufacturing: Dynamic Bonding Strategies for Upcycling Thermoplastics and Thermosets. *Macromol. Rapid Commun.* **2025**, *46*, 2401011.

(29) Nettles, J. A.; Alfarhan, S.; Pascoe, C. A.; Westover, C.; Madsen, M. D.; Sintas, J. I.; Subbiah, A.; Long, T. E.; Jin, K. Functional Upcycling of Polyurethane Thermosets into Value-Added Thermoplastics via

Downloaded from pubs.acs.org/amlcef/article-pdf/8/9/2807/6740807/tz-2026-00833d.pdf by FLORIDA STATE UNIV user on 02 November 2026

https://doi.org/10.1021/acsmaterialslett.6c00833
ACS Materials Lett. 2026, 8, 2807–2816

Small-Molecule Carbamate-Assisted Decross-Linking Extrusion. *JACS Au* **2024**, *4*, 3058–3069.
(30) Tretbar, C. A.; Neal, J. A.; Guan, Z. Direct Silyl Ether Metathesis for Vitrimers with Exceptional Thermal Stability. *J. Am. Chem. Soc.* **2019**, *141*, 16595–16599.
(31) Ge, J.; Caldona, E. B.; Advincula, R. C. Functional Stimuli-Responsive Polymers on Micro- and Nano-Patterned Interfaces. *Polymer* **2025**, *317*, 127958.
(32) Sun, H.; Kabb, C. P.; Sims, M. B.; Sumerlin, B. S. Architecture-Transformable Polymers: Reshaping the Future of Stimuli-Responsive Polymers. *Prog. Polym. Sci.* **2019**, *89*, 61–75.
(33) Bagare, S. V.; Lee, M. J.; Kuehnle, A.; Moore, J. S.; Baur, J. W. Initiator-Driven Tailoring of Reactivity and Inhibition in Frontally Polymerized Dicyclopentadiene-Co-Dihydrofuran Thermosets. *J. Polym. Sci.* **2025**, *63*, 4061–4074.
(34) Cuthbert, T. J.; Li, T.; Speed, A. W. H.; Wulff, J. E. Structure of the Thermally Induced Cross-Link in C-Linked Methyl Ester-Functionalized Polydicyclopentadiene (fPDCPD). *Macromolecules* **2018**, *51*, 2038–2047.
(35) Li, T.; Wulff, J. E. Copolymers of Functionalized and Nonfunctionalized Polydicyclopentadiene. *ACS Appl. Polym. Mater.* **2021**, *3*, 110–115.
(36) Wang, Y.; Zhang, L.; Sun, J.; Bao, J.-B.; Wang, Z.; Ni, L. Dramatic Toughness Enhancement of Polydicyclopentadiene Composites by Incorporating Low Amounts of Vinyl-Functionalized SiO2. *Ind. Eng. Chem. Res.* **2017**, *56*, 4750–4757.
(37) Hu, J.; Gao, Y.; Teng, J.; Li, L.; Zhang, T.; Zheng, S. Recycling of Polydicyclopentadiene Enabled with N-Coordinated Boronic Ester Bonds. *Macromol. Rapid Commun.* **2024**, *45*, 2400169.
(38) Ziaee, M.; Naseri, I.; Johnson, J. W.; Franklin, K. A.; Yourdkhani, M. Frontal Polymerization and Three-Dimensional Printing of Thermoset Polymers with Tunable Thermomechanical Properties. *ACS Appl. Polym. Mater.* **2023**, *5*, 1715–1724.
(39) Kovačič, S.; Slugovc, C. Ring-Opening Metathesis Polymerisation Derived Poly(Dicyclopentadiene) Based Materials. *Mater. Chem. Front.* **2020**, *4*, 2235–2255.
(40) Mol, J. C. Industrial Applications of Olefin Metathesis. *J. Mol. Catal. A: Chem.* **2004**, *213*, 39–45.
(41) Husted, K. E. L.; Shieh, P.; Lundberg, D. J.; Kristufek, S. L.; Johnson, J. A. Molecularly Designed Additives for Chemically Deconstructable Thermosets without Compromised Thermomechanical Properties. *ACS Macro Lett.* **2021**, *10*, 805–810.
(42) Schrock, R. R. Multiple Metal–Carbon Bonds for Catalytic Metathesis Reactions (Nobel Lecture). *Angew. Chem., Int. Ed.* **2006**, *45*, 3748–3759.
(43) Grubbs, R. H. Olefin-Metathesis Catalysts for the Preparation of Molecules and Materials (Nobel Lecture). *Angew. Chem., Int. Ed.* **2006**, *45*, 3760–3765.
(44) Joo, W.; Chen, C. H.; Moerdyk, J. P.; Deschner, R. P.; Bielawski, C. W.; Willson, C. G. Photoinitiated Ring-Opening Metathesis Polymerization. *J. Polym. Sci. Part Polym. Chem.* **2019**, *57*, 1791–1795.
(45) Leguizamon, S. C.; Lyons, K.; Monk, N. T.; Hochrein, M. T.; Jones, B. H.; Foster, J. C. Additive Manufacturing of Degradable Materials via Ring-Opening Metathesis Polymerization (ROMP). *ACS Appl. Mater. Interfaces* **2022**, *14*, 51301–51306.
(46) Leguizamon, S. C.; Monk, N. T.; Hochrein, M. T.; Zapien, E. M.; Yoon, A.; Foster, J. C.; Appelhans, L. N. Photoinitiated Olefin Metathesis and Stereolithographic Printing of Polydicyclopentadiene. *Macromolecules* **2022**, *55*, 8273–8282.
(47) Robertson, I. D.; Yourdkhani, M.; Centellas, P. J.; Aw, J. E.; Ivanoff, D. G.; Goli, E.; Lloyd, E. M.; Dean, L. M.; Sottos, N. R.; Geubelle, P. H.; Moore, J. S.; White, S. R. Rapid Energy-Efficient Manufacturing of Polymers and Composites via Frontal Polymerization. *Nature* **2018**, *557*, 223–227.
(48) Cong, R.; Ban, C.; Li, W.; Li, Y.; Si, G. Thermally Remendable Dynamically Cross-Linked Thermoplastic and Thermoset Materials Directly Synthesized via Ring-Opening Metathesis Polymerization. *CCS Chem.* **2025**, *7*, 3484–3492.
(49) Shieh, P.; Zhang, W.; Husted, K. E. L.; Kristufek, S. L.; Xiong, B.; Lundberg, D. J.; Lem, J.; Veysset, D.; Sun, Y.; Nelson, K. A.; Plata, D. L.; Johnson, J. A. Cleavable Comonomers Enable Degradable, Recyclable Thermoset Plastics. *Nature* **2020**, *583*, 542–547.
(50) Husted, K. E. L.; Brown, C. M.; Shieh, P.; Kevlishvili, I.; Kristufek, S. L.; Zafar, H.; Accardo, J. V.; Cooper, J. C.; Klausen, R. S.; Kulik, H. J.; Moore, J. S.; Sottos, N. R.; Kalow, J. A.; Johnson, J. A. Remolding and Deconstruction of Industrial Thermosets via Carboxylic Acid-Catalyzed Bifunctional Silyl Ether Exchange. *J. Am. Chem. Soc.* **2023**, *145*, 1916–1923.
(51) Liguori, A.; Hakkarainen, M. Designed from Biobased Materials for Recycling: Imine-Based Covalent Adaptable Networks. *Macromol. Rapid Commun.* **2022**, *43*, 2100816.
(52) Schoustra, S. K.; Asadi, V.; Smulders, M. M. J. Probing the Solubility of Imine-Based Covalent Adaptable Networks. *ACS Appl. Polym. Mater.* **2024**, *6*, 79–89.
(53) Taynton, P.; Zhu, C.; Loob, S.; Shoemaker, R.; Pritchard, J.; Jin, Y.; Zhang, W. Re-Healable Polyimine Thermosets: Polymer Composition and Moisture Sensitivity. *Polym. Chem.* **2016**, *7*, 7052–7056.
(54) Saito, K.; Eisenreich, F.; Türel, T.; Tomović, Ž. Closed-Loop Recycling of Poly(Imine-Carbonate) Derived from Plastic Waste and Bio-Based Resources. *Angew. Chem.* **2022**, *134*, e202211806.
(55) Schoustra, S. K.; Kloots, M. H. P., de Heer; Posthuma, J.; Doorn, D., van; Dijksman, J. A.; Smulders, M. M. J. Raman Spectroscopy Reveals Phase Separation in Imine-Based Covalent Adaptable Networks. *Macromolecules* **2022**, *55*, 10341–10355.
(56) Schoustra, S. K.; Dijksman, J. A.; Zuilhof, H.; Smulders, M. M. J. Molecular Control over Vitrimer-like Mechanics – Tuneable Dynamic Motifs Based on the Hammett Equation in Polyimine Materials. *Chem. Sci.* **2021**, *12*, 293–302.
(57) Schoustra, S. K.; Groeneveld, T.; Smulders, M. M. J. The Effect of Polarity on the Molecular Exchange Dynamics in Imine-Based Covalent Adaptable Networks. *Polym. Chem.* **2021**, *12*, 1635–1642.
(58) Belowich, M. E.; Stoddart, J. F. Dynamic Imine Chemistry. *Chem. Soc. Rev.* **2012**, *41*, 2003–2024.
(59) Kim, S.; Rahman, M. A.; Arifuzzaman, M.; Gilmer, D. B.; Li, B.; Wilt, J. K.; Lara-Curzio, E.; Saito, T. Closed-Loop Additive Manufacturing of Upcycled Commodity Plastic through Dynamic Cross-Linking. *Sci. Adv.* **2022**, *8*, eabn6006.
(60) Hoyle, C. E.; Bowman, C. N. Thiol–Ene Click Chemistry. *Angew. Chem., Int. Ed.* **2010**, *49*, 1540–1573.
(61) Lowe, A. B. Thiol-Ene "Click" Reactions and Recent Applications in Polymer and Materials Synthesis. *Polym. Chem.* **2010**, *1*, 17–36.
(62) Lowe, A. B.; Hoyle, C. E.; Bowman, C. N. Thiol - Yne Click Chemistry: A Powerful and Versatile Methodology for Materials Synthesis. *J. Mater. Chem.* **2010**, *20*, 4745–4750.
(63) Zilm, K. W.; Conlin, R. T.; Grant, D. M.; Michl, J. Low-Temperature Carbon-13 Magnetic Resonance of Solids. 1 Alkenes and Cycloalkenes. *J. Am. Chem. Soc.* **1980**, *102*, 6672–6676.
(64) Abadie, M. J.; Dimonie, M.; Couve, C.; Dragutan, V. New Catalysts for Linear Polydicyclopentadiene Synthesis. *Eur. Polym. J.* **2000**, *36*, 1213–1219.
(65) Gong, L.; Liu, K.; Ou, E.; Xu, F.; Lu, Y.; Wang, Z.; Gao, T.; Yang, Z.; Xu, W. ROMP of Acetoxy-Substituted Dicyclopentadiene to a Linear Polymer with a High Tg. *RSC Adv.* **2015**, *5*, 26185–26188.
(66) Raptopoulos, G.; Anyfantis, G. C.; Chriti, D.; Paraskevopoulou, P. Synthesis and Structural Characterization of Poly(Dicyclopentadiene) Gels Obtained with a Novel Ditungsten versus Conventional W and Ru Mononuclear Catalysts. *Inorg. Chim. Acta.* **2017**, *460*, 69–76.
(67) Sarneski, J. E.; Surprenant, H. L.; Molen, F. K.; Reilley, C. N. Chemical Shifts and Protonation Shifts in Carbon-13 Nuclear Magnetic Resonance Studies of Aqueous Amines. *Anal. Chem.* **1975**, *47*, 2116–2124.

Downloaded from pubs.acs.org/amlcef/article-pdf/8/9/2807/6740807/tz-2026-00833d.pdf by FLORIDA STATE UNIV user on 02 November 2026

https://doi.org/10.1021/acsmaterialslett.6c00833
ACS Materials Lett. 2026, 8, 2807–2816

(68) Özeroğlu, B.; Özkan, N. Investigating the Multistep Polymerization Reactions of DCPD with Grubbs' First-Generation Catalyst. *ACS Appl. Polym. Mater.* **2025**, *7*, 6250–6261.
(69) Zhan, Q.; Yang, P. Upgrading of Thermosets and Composites via Sequential Frontal Ring-Opening Metathesis Polymerization and Radical Reactions. *J. Mater. Sci.* **2024**, *59*, 7779–7792.
(70) Flory, P. J.; Rehner, J. Statistical Mechanics of Cross-Linked Polymer Networks II Swelling. *J. Chem. Phys.* **1943**, *11*, 521–526.
(71) Boden, J.; Bowen, C. R.; Buchard, A.; Davidson, M. G.; Norris, C. Understanding the Effects of Cross-Linking Density on the Self-Healing Performance of Epoxidized Natural Rubber and Natural Rubber. *ACS Omega* **2022**, *7*, 15098–15105.
(72) Hiranobe, C. T.; Ribeiro, G. D.; Torres, G. B.; Reis, E. A. P. d.; Cabrera, F. C.; Job, A. E.; Paim, L. L.; Santos, R. J. d. Cross-Linked Density Determination of Natural Rubber Compounds by Different Analytical Techniques. *Mater. Res.* **2021**, *24*, e20210041.
(73) Cornille, A.; Froidevaux, V.; Negrell, C.; Caillol, S.; Boutevin, B. Thiol-Ene Coupling: An Efficient Tool for the Synthesis of New Biobased Aliphatic Amines for Epoxy Curing. *Polymer* **2014**, *55*, 5561–5570.
(74) Zhou, Y.; Wu, F.; Zhu, L.; Geng, Z.; Yang, R.; Zhai, J. Synergistic Effect of Covalent Cross-Linking and Physical Hydrogen Bonding Associations on the Mechanical Properties of Polyurethane Thermoset Elastomers. *J. Appl. Polym. Sci.* **2024**, *141*, e56114.
(75) Prasad, D.; Mitra, N. Noncovalent Interactions in Mechanical Response of Thermoset Epoxy Resin. *J. Phys. Chem. B* **2024**, *128*, 2537–2549.
(76) Snyder, R. L.; Lidston, C. A. L.; Hoe, G. X. D.; Parvulescu, M. J. S.; Hillmyer, M. A.; Coates, G. W. Mechanically Robust and Reprocessable Imine Exchange Networks from Modular Polyester Pre-Polymers. *Polym. Chem.* **2020**, *11*, 5346–5355.
(77) Song, F.; Li, Z.; Jia, P.; Zhang, M.; Bo, C.; Feng, G.; Hu, L.; Zhou, Y. Tunable "Soft and Stiff", Self-Healing, Recyclable, Thermadapt Shape Memory Biomass Polymers Based on Multiple Hydrogen Bonds and Dynamic Imine Bonds. *J. Mater. Chem. A* **2019**, *7*, 13400–13410.
(78) Ward, I. M.; Sweeney, J. Rubber-Like Elasticity. In: *Mechanical Properties of Solid Polymers*. 3rd ed.; John Wiley & Sons, Ltd, **2012**; pp 61–85.
(79) Lin, D. C.; Douglas, J. F.; Horkay, F. Development of Minimal Models of the Elastic Properties of Flexible and Stiff Polymer Networks with Permanent and Thermoreversible Cross-Links. *Soft Matter* **2010**, *6*, 3548–3561.
(80) Liu, Y.; Tang, Z.; Chen, J.; Xiong, J.; Wang, D.; Wang, S.; Wu, S.; Guo, B. Tuning the Mechanical and Dynamic Properties of Imine Bond Crosslinked Elastomeric Vitrimers by Manipulating the Crosslinking Degree. *Polym. Chem.* **2020**, *11*, 1348–1355.
(81) Marco-Dufort, B.; Tibbitt, M. W. Design of Moldable Hydrogels for Biomedical Applications Using Dynamic Covalent Boronic Esters. *Mater. Today Chem.* **2019**, *12*, 16–33.
(82) Winne, J. M.; Leibler, L.; Du Prez, F. E. Dynamic Covalent Chemistry in Polymer Networks: A Mechanistic Perspective. *Polym. Chem.* **2019**, *10*, 6091–6108.
(83) Kong, V. A.; Staunton, T. A.; Laaser, J. E. Effect of Cross-Link Homogeneity on the High-Strain Behavior of Elastic Polymer Networks. *Macromolecules* **2024**, *57*, 4670–4679.
(84) Lee, H.; Kim, J.; Lee, M.; Kang, J. Dynamic Bond Chemistry in Soft Materials: Bridging Adaptability and Mechanical Robustness. *Chem. Rev.* **2025**, *125*, 11379–11425.
(85) Babkina, N. V.; Lipatov, Y. S.; Alekseeva, T. T. Damping Properties of Composites Based on Interpenetrating Polymer Networks Formed in the Presence of Compatibilizing Additives. *Mech. Compos. Mater.* **2006**, *42*, 385–392.
(86) Hayashi, M.; Ricarte, R. G. Towards the next Development of Vitrimers: Recent Key Topics for the Practical Application and Understanding of the Fundamental Physics. *Prog. Polym. Sci.* **2025**, *170*, 102026.
(87) Santiago, D.; Guzmán, D.; Padilla, J.; Verdugo, P.; De la Flor, S.; Serra, À. Recyclable and Reprocessable Epoxy Vitrimer Adhesives. *ACS Appl. Polym. Mater.* **2023**, *5*, 2006–2015.
(88) Liu, J.; Liu, X.; Cui, X.; Qin, J.; Shi, M.; Wang, D.; Liang, L.; Yang, C. Imine-Containing Epoxy Vitrimer Cured by Active Ester: Properties and Theoretical Analysis. *ACS Appl. Polym. Mater.* **2023**, *5*, 10042–10052.
(89) Guerre, M.; Taplan, C.; Winne, J. M.; Prez, F. E. D. Vitrimers: Directing Chemical Reactivity to Control Material Properties. *Chem. Sci.* **2020**, *11*, 4855–4870.
(90) Wu, S.; Chen, Q. Advances and New Opportunities in the Rheology of Physically and Chemically Reversible Polymers. *Macromolecules* **2022**, *55*, 697–714.
(91) Scheutz, G. M.; Lessard, J. J.; Sims, M. B.; Sumerlin, B. S. Adaptable Crosslinks in Polymeric Materials: Resolving the Intersection of Thermoplastics and Thermosets. *J. Am. Chem. Soc.* **2019**, *141*, 16181–16196.
(92) Ogden, W. A.; Guan, Z. Recyclable, Strong, and Highly Malleable Thermosets Based on Boroxine Networks. *J. Am. Chem. Soc.* **2018**, *140*, 6217–6220.
(93) Lessard, J. J.; Scheutz, G. M.; Sung, S. H.; Lantz, K. A.; Epps, T. H.; Sumerlin, B. S. Block Copolymer Vitrimers. *J. Am. Chem. Soc.* **2020**, *142*, 283–289.
(94) Ge, S.; Tsao, Y.-H.; Evans, C. M. Polymer Architecture Dictates Multiple Relaxation Processes in Soft Networks with Two Orthogonal Dynamic Bonds. *Nat. Commun.* **2023**, *14*, 7244.
(95) Elling, B. R.; Dichtel, W. R. Reprocessable Cross-Linked Polymer Networks: Are Associative Exchange Mechanisms Desirable?. *ACS Cent. Sci.* **2020**, *6*, 1488–1496.
(96) Dhers, S.; Vantomme, G.; Avérous, L. A Fully Bio-Based Polyimine Vitrimer Derived from Fructose. *Green Chem.* **2019**, *21*, 1596–1601.
(97) Hubbard, A. M.; Ren, Y.; Sarvestani, A.; Picu, C. R.; Varshney, V.; Nepal, D. Thermomechanical Analysis (TMA) of Vitrimers. *Polym. Test.* **2023**, *118*, 107877.
(98) Yang, Y.; Zhang, S.; Zhang, X.; Gao, L.; Wei, Y.; Ji, Y. Detecting Topology Freezing Transition Temperature of Vitrimers by AIE Luminogens. *Nat. Commun.* **2019**, *10*, 3165.
(99) Denissen, W.; Winne, J. M.; Prez, F. E. D. Vitrimers: Permanent Organic Networks with Glass-like Fluidity. *Chem. Sci.* **2016**, *7*, 30–38.
(100) Morici, E.; Dintcheva, N. T. Recycling of Thermoset Materials and Thermoset-Based Composites: Challenge and Opportunity. *Polymers* **2022**, *14*, 4153.
(101) Roig, A.; Hidalgo, P.; Ramis, X.; Flor, S., De la; Serra, À. Vitrimeric Epoxy-Amine Polyimine Networks Based on a Renewable Vanillin Derivative. *ACS Appl. Polym. Mater.* **2022**, *4*, 9341–9350.
(102) Webber, M. J.; Tibbitt, M. W. Dynamic and Reconfigurable Materials from Reversible Network Interactions. *Nat. Rev. Mater.* **2022**, *7*, 541–556.
(103) Memon, H.; Wei, Y.; Zhang, L.; Jiang, Q.; Liu, W. An Imine-Containing Epoxy Vitrimer with Versatile Recyclability and Its Application in Fully Recyclable Carbon Fiber Reinforced Composites. *Compos. Sci. Technol.* **2020**, *199*, 108314.
(104) Memon, H.; Liu, H.; Rashid, M. A.; Chen, L.; Jiang, Q.; Zhang, L.; Wei, Y.; Liu, W.; Qiu, Y. Vanillin-Based Epoxy Vitrimer with High Performance and Closed-Loop Recyclability. *Macromolecules* **2020**, *53*, 621–630.
(105) Luo, C.; Liu, X.; Yang, W.; Wang, Y.; Wang, J.; Lin, J.; Zhang, L.; Ruan, J.; He, S. Multirecyclable, Self-Healable, Chemically Degradable, and High-Strength Epoxy Vitrimers Containing Tailorable Imine Bonds. *Ind. Eng. Chem. Res.* **2025**, *64*, 4685–4693.
(106) Hubbard, A. M.; Ren, Y.; Sarvestani, A.; Konkolewicz, D.; Picu, C. R.; Roy, A. K.; Varshney, V.; Nepal, D. Recyclability of Vitrimer Materials: Impact of Catalyst and Processing Conditions. *ACS Omega* **2022**, *7*, 29125–29134.
(107) Tol, J. J. B., van der; Hafeez, S.; Bänziger, A. P. G.; Su, H.; Heuts, J. P. A.; Meijer, E. W.; Vantomme, G. Supramolecular Polymer

Downloaded from pubs.acs.org/amlcef/article-pdf/8/9/2807/6740807/tz-2026-00833d.pdf by FLORIDA STATE UNIV user on 02 November 2026

https://doi.org/10.1021/acsmaterialslett.6c00833
ACS Materials Lett. 2026, 8, 2807−2816

Additives as Repairable Reinforcements for Dynamic Covalent Networks. *Adv. Mater.* **2024**, *36*, 2410723.
(108) Satheesh Kumar, B.; Robert, T. M.; Roshith, K. R.; Mathew, D.; Santhosh Kumar, K. S. Epoxy-Anhydride Vitrimers: Reprocessability via Facile Transesterification. *Next Mater.* **2025**, *8*, 100690.
(109) Islam, S.; Bhat, G. Progress and Challenges in Self-Healing Composite Materials. *Mater. Adv.* **2021**, *2*, 1896–1926.
(110) Yamaguchi, M.; Ono, S.; Terano, M. Self-Repairing Property of Polymer Network with Dangling Chains. *Mater. Lett.* **2007**, *61*, 1396–1399.
(111) Yang, W.; Ding, H.; Zhou, W.; Liu, T.; Xu, P.; Puglia, D.; Kenny, J. M.; Ma, P. Design of Inherent Fire Retarding and Degradable Bio-Based Epoxy Vitrimer with Excellent Self-Healing and Mechanical Reprocessability. *Compos. Sci. Technol.* **2022**, *230*, 109776.
(112) Peng, J.; Xie, S.; Liu, T.; Wang, D.; Ou, R.; Guo, C.; Wang, Q.; Liu, Z. High-Performance Epoxy Vitrimer with Superior Self-Healing, Shape-Memory, Flame Retardancy, and Antibacterial Properties Based on Multifunctional Curing Agent. *Compos. Part B Eng.* **2022**, *242*, 110109.
(113) Rashid, M. A.; Hasan, M. N.; Kafi, M. A. Synthesis of Novel Vanillin-Amine Hardeners Fully Derived from Renewable Bio Feedstocks and Their Curing with Epoxy Resins to Produce Recyclable Reprocessable Vitrimers. *Heliyon* **2023**, *9*, e16062.
(114) Liu, X.; Liang, L.; Lu, M.; Song, X.; Liu, H.; Chen, G. Water-Resistant Bio-Based Vitrimers Based on Dynamic Imine Bonds: Self-Healability, Remodelability and Ecofriendly Recyclability. *Polymer* **2020**, *210*, 123030.

Downloaded from pubs.acs.org/amlcef/article-pdf/8/9/2807/6740807/lz-2026-00833d.pdf by FLORIDA STATE UNIV user on 02 November 2026

https://doi.org/10.1021/acsmaterialslett.6c00833
ACS Materials Lett. 2026, 8, 2807−2816